

# Crystal structure of bis(tetramethylthiourea- $\kappa$ S)-bis(thiocyanato- $\kappa$ N)nickel(II)

Aleksej Jochim,\* Rastko Radulovic, Inke Jess and Christian Näther

Institut für Anorganische Chemie, Christian-Albrechts-Universität Kiel, Max-Eyth-Str. 2, D-24118 Kiel, Germany.

\*Correspondence e-mail: ajochim@ac.uni-kiel.de

Received 29 October 2020

Accepted 13 November 2020

Edited by B. Therrien, University of Neuchâtel, Switzerland

**Keywords:** crystal structure; nickel thiocyanate; tetramethylthiourea; discrete complexes; thermal properties.

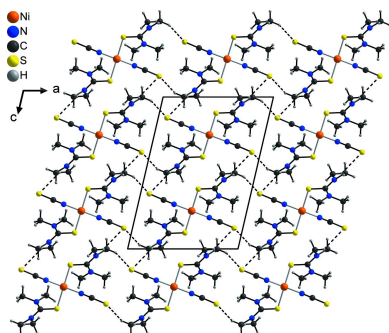
**CCDC reference:** 2044233

**Supporting information:** this article has supporting information at journals.iucr.org/e

In the course of our investigations regarding transition-metal thiocyanates with thiourea derivatives, the title compound,  $[\text{Ni}(\text{NCS})_2(\text{C}_5\text{H}_{12}\text{N}_2\text{S})_2]$ , was obtained. The asymmetric unit consists of one thiocyanate anion and one tetramethylthiourea molecule on general positions, as well as one  $\text{Ni}^{\text{II}}$  cation that is located on a twofold rotational axis. In this compound, discrete complexes are formed in which the  $\text{Ni}^{\text{II}}$  cations are surrounded by two *trans*-N-bonding thiocyanate anions as well as two *trans*-S-bonding tetramethylthiourea molecules within a distorted square-planar coordination geometry. The discrete complexes are linked by pairs of weak C—H $\cdots$ S hydrogen bonds between the thiocyanate S and one of the tetramethylthiourea methyl hydrogen atoms into chains along the crystallographic *a*- and *c*-axis directions, which are combined into layers parallel to the *ac* plane. X-ray powder diffraction proves that a pure crystalline phase was obtained and measurements using thermogravimetry and differential thermoanalysis reveal that the compound decomposes at about 408 K, where all tetramethylthiourea molecules are lost.

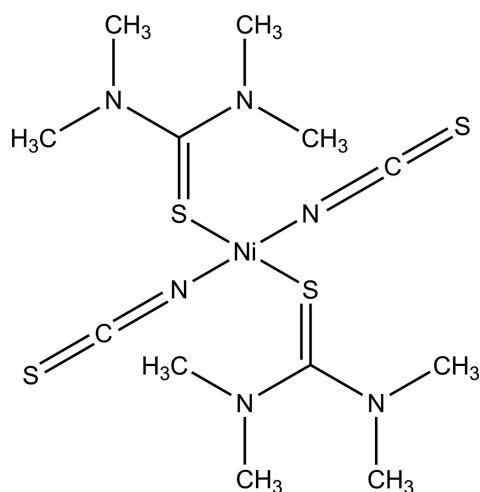
## 1. Chemical context

Many thiocyanate coordination compounds are reported in the literature, which mostly consist of discrete complexes containing non-bridging N-terminally coordinated thiocyanate anions, while compounds in which the metal cations are bridged by these anionic ligands are comparatively rare. Despite this fact, a variety of coordination modes can be found for bridging thiocyanate anions, which leads to metal–thiocyanate networks with different dimensionalities and topologies (Wöhlert *et al.*, 2014; Lin, 2008; Li *et al.*, 2014; Suckert *et al.*, 2016). If these compounds contain paramagnetic metal cations, they are of special interest, because thiocyanate anions can mediate magnetic exchange and thus cooperative magnetic phenomena can be expected (Palion-Gazda *et al.*, 2015; Mekuimemba *et al.*, 2018; Mousavi *et al.*, 2020; Rams *et al.*, 2020; Mautner *et al.*, 2018). Our interest focuses mainly on transition-metal thiocyanates with the general composition  $[\text{M}(\text{NCS})_2(\text{coligand})_2]_n$  with  $M = \text{Mn}^{\text{II}}$ ,  $\text{Fe}^{\text{II}}$ ,  $\text{Co}^{\text{II}}$  or  $\text{Ni}^{\text{II}}$  that consist of linear chains, in which the metal cations are connected by pairs of N- and S-bonding thiocyanate anions into centrosymmetric  $M_2(\text{NCS})_2$  units, while the remaining sites of the coordination octahedron are occupied by neutral coligands forming a coordination environment in which all ligands are *trans* (Wöhlert *et al.*, 2014; Werner *et al.*, 2014, 2015; Prananto *et al.*, 2017). In this context, it is noted that the  $\text{Co}^{\text{II}}$  compounds are of special interest, because either ferromagnetic behavior or a slow relaxation of the magnetization is observed (Werner *et al.*, 2015; Neumann *et al.*, 2019; Rams *et*



OPEN ACCESS

*al.*, 2017, 2020). Besides these chain compounds with an all-*trans* coordination environment, several other isomers with different *cis-cis-trans* arrangements of the ligands can be found in which either the coligand, the N-bonding or the S-bonding thiocyanate are *trans*, while the other ligands are *cis* (Maji *et al.*, 2001; Shi *et al.*, 2007; Rams *et al.*, 2017). For most of these compounds, corrugated chains are observed in which the magnetic exchange is low or negligible (Böhme *et al.*, 2020; Jochim *et al.*, 2018). In the case of  $[M(\text{NCS})_2(4\text{-chloropyridine})_2]_n$  ( $M = \text{Co}, \text{Ni}$ ), two isomeric compounds are observed that contain either linear or corrugated chains, which allowed investigations on the influence of the chain geometry on the magnetic behavior, because both compounds contain the same coligand and thus all differences in the magnetic behavior can be attributed to the structural changes (Böhme *et al.*, 2020; Jochim *et al.*, 2018).



However, to investigate the magnetic properties of transition-metal thiocyanate compounds in more detail, the influence of the coligands on the structural and magnetic behavior must be investigated systematically. Most of these compounds contain N-donor coligands, whereas compounds with, for example, O- or S-donor coligands are rare (Groom *et al.*, 2016; Amzel *et al.*, 1969; Shurdha, *et al.*, 2013). This is the reason why we became interested in transition-metal thiocyanate compounds with thiourea derivatives, where a few compounds have been reported for which either octahedral (Amzel *et al.*, 1969) or tetrahedral complexes (Jochim *et al.*, 2020*a,b*) are observed. Furthermore, some polymeric compounds have been reported in which the metal cations are connected by either the coligands (Nardelli *et al.*, 1966*a*) or the thiocyanate anions into chains (Nardelli *et al.*, 1966*b*; Jochim *et al.*, 2020*c*). In the course of our systematic investigations we became interested in tetramethylthiourea as coligand, which upon reaction with nickel thiocyanate leads to the formation of the title compound  $[\text{Ni}(\text{NCS})_2(\text{C}_5\text{H}_{12}\text{N}_2\text{S})_2]$  that consists of discrete complexes, in which the thiocyanate anions are N-terminally coordinated. Phase pure powders of the title compound could easily be obtained, which is confirmed by X-ray powder diffraction (Fig. S1 in the supporting information). The C–N stretching band of the thiocyanate anion can be found at  $2080\text{ cm}^{-1}$ , which proves the presence of terminally

**Table 1**  
Selected geometric parameters ( $\text{\AA}$ ,  $^\circ$ ).

Ni1–N1	1.844 (3)	Ni1–S11	2.2259 (7)
N1–Ni1–N1 <sup>i</sup>	167.47 (16)	N1 <sup>i</sup> –Ni1–S11	93.93 (8)
N1–Ni1–S11	86.80 (8)	S11 <sup>i</sup> –Ni1–S11	173.26 (5)

Symmetry code: (i)  $-x + 1, y, -z + \frac{3}{2}$ .

ally bonded thiocyanate anions, in accordance with the results from single crystal X-ray diffraction (Fig. S2). Investigation of the thermal behavior of the title compound shows that it decomposes at about 408 K in one discrete step of 59.0%, which is in agreement with the mass loss calculated for the loss of all coligand molecules of 60.2% (Fig. S3).

## 2. Structural commentary

The asymmetric unit consists of one  $\text{Ni}^{\text{II}}$  cation that is located on a twofold rotational axis as well as one thiocyanate anion and one tetramethylthiourea molecule, which both occupy general positions. Each  $\text{Ni}^{\text{II}}$  cation is fourfold coordinated by two *trans* N-binding thiocyanate anions and two *trans* S-binding tetramethylthiourea molecules into discrete complexes. (Fig. 1). The Ni–N bonds are much shorter than the Ni–S bonds and from the angles it is obvious that the Ni cation is in a square-planar coordination geometry (Table 1). Furthermore, a strong deviation from the ideal angles is found in the coordination environment of the Ni cation, which can probably be attributed to the relatively bulky  $\text{NMe}_2$  groups of the tetramethylthiourea molecules. This is most pronounced in the N–Ni–N angle, which amounts to  $167.47(16)^\circ$ . In contrast, for the S–Ni–S angle a smaller deviation with a value of  $173.26(5)^\circ$  can be found. The tetramethylthiourea molecules are twisted relative to each other with a

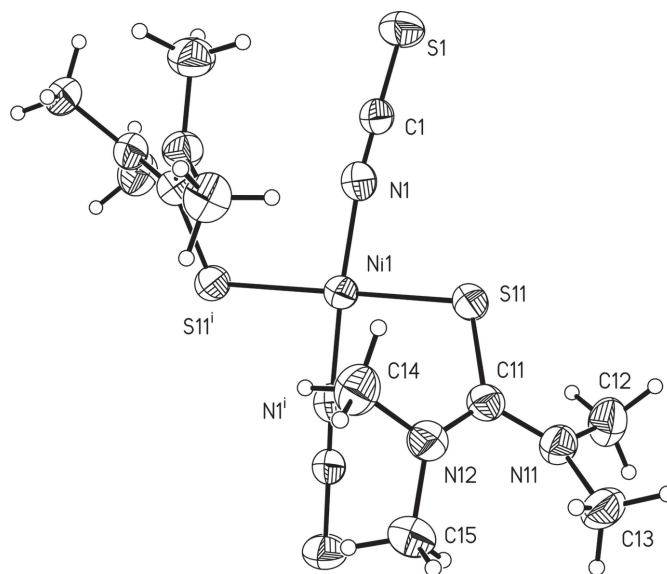


**Figure 1**  
View of the asymmetric unit of the title compound with atom labeling and displacement ellipsoids drawn at the 50% probability level. Symmetry transformations used to generate equivalent atoms: (i)  $-x + 1, y, -z + \frac{3}{2}$ .

**Table 2**  
Hydrogen-bond geometry (Å, °).

$D-H\cdots A$	$D-H$	$H\cdots A$	$D\cdots A$	$D-H\cdots A$
$C12-H12B\cdots S1^{ii}$	0.98	3.01	3.821 (3)	140
$C13-H13C\cdots S1^{iii}$	0.98	2.93	3.798 (3)	148

Symmetry codes: (ii)  $-x + 1, -y, -z + 1$ ; (iii)  $x + 1, y, z$ .

$C=S\cdots S=C$  torsion angle of  $135.0(2)^\circ$ . Furthermore, while the thiourea unit of each tetramethylthiourea ligand is planar, both  $NMe_2$  groups are rotated out of this plane by angles of  $28.8(2)$  and  $27.3(2)^\circ$ .

### 3. Supramolecular features

In the crystal structure of the title compound, the discrete complexes are linked by two crystallographically different intermolecular  $C-H\cdots S$  hydrogen bonds between the thiocyanate S atom S1 and the methyl hydrogen atoms H13C and H12C of the tetramethylthiourea molecule. In both cases, each two neighbouring complexes are linked into pairs containing 18-membered rings that are located on centers of inversion (Fig. 2 and Table 2). These pairs are further linked into chains, which for the hydrogen bonds between S1 and H13C proceed along the crystallographic  $a$ -axis direction and for those between S1 and H12b along the  $c$ -axis direction (Fig. 2). These two chains condense into layers parallel to the  $ac$  plane by centrosymmetric pairs of both crystallographically different  $C-H\cdots S$  hydrogen bonds (Fig. 3).

### 4. Database survey

In the Cambridge Crystallographic Database (CSD, Version 5.41, last update May 2020; Groom *et al.*, 2016) no transition-metal thiocyanate compounds with tetramethylthiourea are reported, but one such compound with cobalt was published recently (Jochim *et al.*, 2020*b*). In this compound, discrete

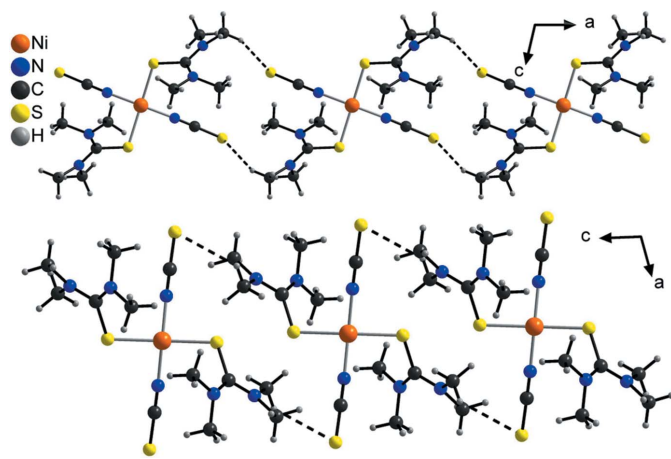


**Figure 2**  
Crystal structure of the title compound with view of the two different chains formed by intermolecular  $C-H\cdots S$  hydrogen bonding between S1 and H13C (top) and between S1 and H12B (bottom). Intermolecular  $C-H\cdots S$  hydrogen bonding is shown as dashed lines.

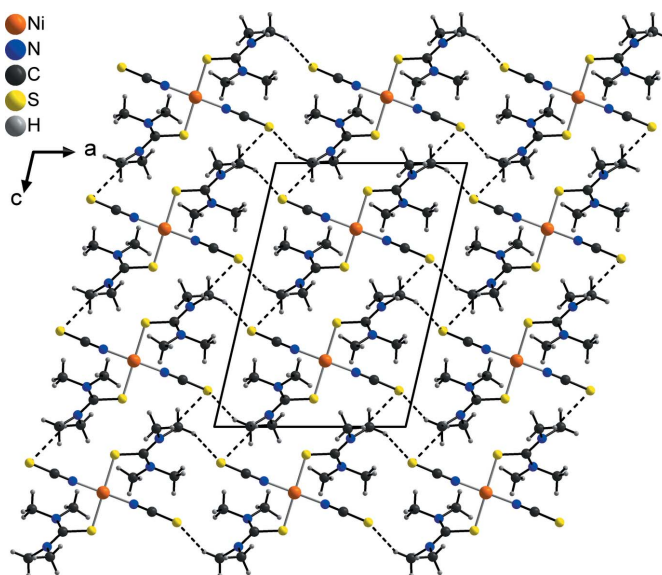


**Figure 3**  
Crystal structure of the title compound with view along the crystallographic  $b$  axis and intermolecular  $C-H\cdots S$  hydrogen bonding shown as dashed lines.

tetrahedral complexes are found in which the metal cations are coordinated by two N-bonding thiocyanate anions and two S-bonding tetramethylthiourea molecules. Several compounds with transition-metal cations and tetramethylthiourea are reported in the CSD, of which two contain nickel cations. Both consist of discrete binuclear complexes in which the metal cations are connected by thiolate ligands. These complexes contain either two  $Ni^{II}$  cations with a square-planar coordination geometry (Ito *et al.*, 2009) or one  $Ni^{II}$  and one  $Fe^{II}$  cation with square-pyramidal and octahedral coordination geometries (Ohki *et al.*, 2008), respectively. Several  $Ni(NCS)_2$  compounds with other thiourea derivatives are also found, including polymeric compounds such as  $[Ni(NCS)_2(\text{ethylene-thiourea})_2]_n$  (Nardelli *et al.*, 1966*b*) and discrete complexes like  $[Ni(NCS)_2(N,N'\text{-diethylthiourea})_4]$  (Amzel *et al.*, 1969), but only one of those contains nickel cations with a square-planar coordination geometry (Leovac *et al.*, 1995).

### 5. Synthesis and crystallization

#### General

$Ni(NCS)_2$  was synthesized using a procedure described in Jochim *et al.* (2018). The reagents  $NiSO_4\cdot 6H_2O$  and  $Ba(NCS)_2\cdot 3H_2O$ , which were used for this, were obtained from Merck and Alfa Aesar, respectively.

#### Synthesis

To synthesize a powder sample, a mixture of  $Ni(NCS)_2$  (0.50 mmol, 87.4 mg) and tetramethylthiourea (1.00 mmol, 132.2 mg) was stirred in 0.5 mL of ethanol for one day. The black residue was filtered off and washed with *n*-heptane. Single crystals were grown by slow evaporation of the filtrate obtained from a similar reaction. In this case,  $Ni(NCS)_2$  (0.25 mmol, 43.7 mg) and tetramethylthiourea (1.00 mmol,

**Table 3**  
Experimental details.

Crystal data	
Chemical formula	[Ni(NCS) <sub>2</sub> (C <sub>5</sub> H <sub>12</sub> N <sub>2</sub> S) <sub>2</sub> ]
<i>M<sub>r</sub></i>	439.32
Crystal system, space group	Monoclinic, <i>P2/c</i>
Temperature (K)	200
<i>a</i> , <i>b</i> , <i>c</i> (Å)	10.7245 (3), 6.2050 (3), 15.1579 (5)
β (°)	103.140 (3)
<i>V</i> (Å <sup>3</sup> )	982.28 (6)
<i>Z</i>	2
Radiation type	Mo <i>K</i> α
μ (mm <sup>-1</sup> )	1.42
Crystal size (mm)	0.12 × 0.09 × 0.07
Data collection	
Diffractometer	Stoe IPDS2
Absorption correction	Numerical ( <i>X-RED</i> and <i>X-SHAPE</i> ; Stoe & Cie, 2002)
<i>T<sub>min</sub></i> , <i>T<sub>max</sub></i>	0.716, 0.874
No. of measured, independent and observed [ <i>I</i> > 2σ( <i>I</i> )] reflections	9982, 1945, 1607
<i>R<sub>int</sub></i>	0.070
(sin θ/λ) <sub>max</sub> (Å <sup>-1</sup> )	0.617
Refinement	
<i>R</i> [ <i>F</i> <sup>2</sup> > 2σ( <i>F</i> <sup>2</sup> )], <i>wR</i> ( <i>F</i> <sup>2</sup> ), <i>S</i>	0.038, 0.098, 1.05
No. of reflections	1945
No. of parameters	109
H-atom treatment	H-atom parameters constrained
Δρ <sub>max</sub> , Δρ <sub>min</sub> (e Å <sup>-3</sup> )	0.39, -0.36

Computer programs: *X-AREA* (Stoe & Cie, 2002), *SHELXS97* (Sheldrick, 2008), *SHELXL2018/3* (Sheldrick, 2015), *XP* (Sheldrick, 2008), *DIAMOND* (Brandenburg & Putz, 1999) and *publCIF* (Westrip, 2010).

132.3 mg) were reacted in 0.5 mL of *n*-butanol for one day, after which the residue was filtered off. Elemental analysis calculated for C<sub>12</sub>H<sub>24</sub>N<sub>6</sub>NiS<sub>4</sub> (439.32 g mol<sup>-1</sup>) C 32.81, H 5.51, N 19.13, S 29.20, found: C 32.77, H 5.42, N 19.07, S 29.18. IR (ATR): ν<sub>max</sub> = 3025 (*w*), 3008 (*w*), 2954 (*w*), 2926 (*w*), 2164 (*w*), 2080 (*s*), 1555 (*s*), 1492 (*m*), 1461 (*m*), 1441 (*m*), 1415 (*w*), 1378 (*s*), 1259 (*m*), 1209 (*w*), 1156 (*s*), 1109 (*s*), 1100 (*s*), 1060 (*m*), 1055 (*m*), 941 (*w*), 878 (*s*), 845 (*s*), 653 (*m*), 612 (*m*), 490 (*m*), 478 (*m*), 468 (*m*), 408 (*m*) cm<sup>-1</sup>.

### Experimental details

Elemental analysis was performed using an EURO EA elemental analyzer fabricated by EURO VECTOR Instruments. The IR spectrum was measured using an ATI Mattson Genesis Series FTIR Spectrometer, control software: *WINFIRST*, from ATI Mattson. The XRPD measurements were performed with Cu *K*α<sub>1</sub> radiation (λ = 1.540598 Å) using a Stoe Transmission Powder Diffraction System (STADI P) that is equipped with a MYTHEN 1K detector and a Johansson-type Ge(111) monochromator. DTA–TG measurements were performed in a dynamic nitrogen atmosphere (5 NL h<sup>-1</sup>) in Al<sub>2</sub>O<sub>3</sub> crucibles using a STA-PT 1000 thermobalance from Linseis. The instrument was calibrated using standard reference materials.

## 6. Refinement

Crystal data, data collection and structure refinement details are summarized in Table 3. All non-hydrogen atoms were

refined with anisotropic displacement parameters. The C-bound H atoms were positioned with idealized geometry (C–H = 0.98 Å) allowing them to rotate, but not to tip and refined isotropically with *U*<sub>iso</sub>(H) = 1.5*U*<sub>eq</sub>(C).

## Acknowledgements

We thank Professor Dr Wolfgang Bensch for access to his experimental facilities.

## Funding information

This project was supported by the Deutsche Forschungsgemeinschaft (Project No. NA 720/5–2) and the State of Schleswig-Holstein.

## References

- Amzel, L. M., Baggio, S. & Becka, L. N. (1969). *J. Chem. Soc. A*, pp. 2066–2073.
- Böhme, M., Jochim, A., Rams, M., Lohmiller, T., Suckert, S., Schnegg, A., Plass, W. & Näther, C. (2020). *Inorg. Chem.* **59**, 5325–5338.
- Brandenburg, K. & Putz, H. (1999). *DIAMOND*. Crystal Impact GbR, Bonn, Germany.
- Groom, C. R., Bruno, I. J., Lightfoot, M. P. & Ward, S. C. (2016). *Acta Cryst.* **B72**, 171–179.
- Ito, M., Kotera, M., Song, Y., Matsumoto, T. & Tatsumi, K. (2009). *Inorg. Chem.* **48**, 1250–1256.
- Jochim, A., Lohmiller, T., Rams, M., Böhme, M., Ceglarska, M., Schnegg, A., Plass, W. & Näther, C. (2020c). *Inorg. Chem.* **59**, 8971–8982.
- Jochim, A., Radulovic, R., Jess, I. & Näther, C. (2020a). *Acta Cryst.* **E76**, 1373–1377.
- Jochim, A., Radulovic, R., Jess, I. & Näther, C. (2020b). *Acta Cryst.* **E76**, 1476–1481.
- Jochim, A., Rams, M., Neumann, T., Wellm, C., Reinsch, H., Wójtowicz, G. M. & Näther, C. (2018). *Eur. J. Inorg. Chem.* pp. 4779–4789.
- Leovac, V. M., Češljević, V. I., Argay, G., Kálmán, A. & Ribár, B. (1995). *J. Coord. Chem.* **34**, 357–364.
- Li, L., Chen, S., Zhou, R.-M., Bai, Y. & Dang, D.-B. (2014). *Spectrochim. Acta Part A*, **120**, 401–404.
- Lin, H.-W. (2008). *Acta Cryst.* **E64**, m295.
- Maji, T. K., Laskar, I. R., Mostafa, G., Welch, A. J., Mukherjee, P. S. & Chaudhuri, N. R. (2001). *Polyhedron*, **20**, 651–655.
- Mautner, F. A., Traber, M., Fischer, R. C., Torvisco, A., Reichmann, K., Speed, S., Vicente, R. & Massoud, S. S. (2018). *Polyhedron*, **154**, 436–442.
- Mekuimemba, C. D., Conan, F., Mota, A. J., Palacios, M. A., Colacio, E. & Triki, S. (2018). *Inorg. Chem.* **57**, 2184–2192.
- Mousavi, M., Duhayon, C., Bretosh, K., Béreau, V. & Sutter, J. P. (2020). *Inorg. Chem.* **59**, 7603–7613.
- Nardelli, M., Gasparri, G. F., Battistini, G. G. & Domiano, P. (1966a). *Acta Cryst.* **20**, 349–353.
- Nardelli, M., Gasparri, G. F., Musatti, A. & Manfredotti, A. (1966b). *Acta Cryst.* **21**, 910–919.
- Neumann, T., Rams, M., Tomkowicz, Z., Jess, I. & Näther, C. (2019). *Chem. Commun.* **55**, 2652–2655.
- Ohki, Y., Yasumura, K., Kuge, K., Tanino, S., Ando, M., Li, Z. & Tatsumi, K. (2008). *Proc. Natl Acad. Sci. USA*, **105**, 7652–7657.
- Palion-Gazda, J., Machura, B., Lloret, F. & Julve, M. (2015). *Cryst. Growth Des.* **15**, 2380–2388.
- Prananto, Y. P., Urbatsch, A., Moubaraki, B., Murray, K. S., Turner, D. R., Deacon, G. B. & Batten, S. R. (2017). *Aust. J. Chem.* **70**, 516–528.

- Rams, M., Jochim, A., Böhme, M., Lohmiller, T., Ceglarska, M., Rams, M. M., Schnegg, A., Plass, W. & Näther, C. (2020). *Chem. Eur. J.* **26**, 2837–2851.
- Rams, M., Tomkowicz, Z., Böhme, M., Plass, W., Suckert, S., Werner, J., Jess, I. & Näther, C. (2017). *Phys. Chem. Chem. Phys.* **19**, 3232–3243.
- Sheldrick, G. M. (2008). *Acta Cryst.* **A64**, 112–122.
- Sheldrick, G. M. (2015). *Acta Cryst.* **C71**, 3–8.
- Shi, J.-M., Chen, J.-N., Wu, C.-J. & Ma, J.-P. (2007). *J. Coord. Chem.* **60**, 2009–2013.
- Shurdha, E., Moore, C. E., Rheingold, A. L., Lapidus, S. H., Stephens, P. W., Arif, A. M. & Miller, J. S. (2013). *Inorg. Chem.* **52**, 10583–10594.
- Stoe & Cie (2002). *X-AREA, X-RED and X-SHAPE*. Stoe & Cie, Darmstadt, Germany.
- Suckert, S., Rams, M., Böhme, M., Germann, L. S., Dinnebier, R. E., Plass, W., Werner, J. & Näther, C. (2016). *Dalton Trans.* **45**, 18190–18201.
- Werner, J., Neumann, T. & Näther, C. (2014). *Z. Anorg. Allg. Chem.* **640**, 2839–2846.
- Werner, J., Tomkowicz, Z., Rams, M., Ebbinghaus, S. G., Neumann, T. & Näther, C. (2015). *Dalton Trans.* **44**, 14149–14158.
- Westrip, S. P. (2010). *J. Appl. Cryst.* **43**, 920–925.
- Wöhlert, S., Runčevski, T., Dinnebier, R. E., Ebbinghaus, S. G. & Näther, C. (2014). *Cryst. Growth Des.* **14**, 1902–1913.

## supporting information

*Acta Cryst.* (2020). E76, 1841-1845 [https://doi.org/10.1107/S2056989020015121]

## Crystal structure of bis(tetramethylthiourea- $\kappa$ S)bis(thiocyanato- $\kappa$ N)nickel(II)

Aleksej Jochim, Rastko Radulovic, Inke Jess and Christian Näther

### Computing details

Data collection: *X-AREA* (Stoe & Cie, 2002); cell refinement: *X-AREA* (Stoe & Cie, 2002); data reduction: *X-AREA* (Stoe & Cie, 2002); program(s) used to solve structure: *SHELXS97* (Sheldrick, 2008); program(s) used to refine structure: *SHELXL2018/3* (Sheldrick, 2015); molecular graphics: *XP* (Sheldrick, 2008) and *DIAMOND* (Brandenburg & Putz, 1999); software used to prepare material for publication: *publCIF* (Westrip, 2010).

### Bis(tetramethylthiourea- $\kappa$ S)bis(thiocyanato- $\kappa$ N)nickel(II)

#### Crystal data

[Ni(NCS)<sub>2</sub>(C<sub>3</sub>H<sub>12</sub>N<sub>2</sub>S)<sub>2</sub>]

$M_r = 439.32$

Monoclinic, *P2/c*

$a = 10.7245$  (3) Å

$b = 6.2050$  (3) Å

$c = 15.1579$  (5) Å

$\beta = 103.140$  (3)°

$V = 982.28$  (6) Å<sup>3</sup>

$Z = 2$

$F(000) = 460$

$D_x = 1.485$  Mg m<sup>-3</sup>

Mo  $K\alpha$  radiation,  $\lambda = 0.71073$  Å

Cell parameters from 9982 reflections

$\theta = 2.0$ – $26.0$ °

$\mu = 1.42$  mm<sup>-1</sup>

$T = 200$  K

Block, black

$0.12 \times 0.09 \times 0.07$  mm

#### Data collection

Stoe IPDS-2  
diffractometer

$\omega$  scans

Absorption correction: numerical  
(X-Red and X-Shape; Stoe & Cie, 2002)

$T_{\min} = 0.716$ ,  $T_{\max} = 0.874$

9982 measured reflections

1945 independent reflections

1607 reflections with  $I > 2\sigma(I)$

$R_{\text{int}} = 0.070$

$\theta_{\max} = 26.0$ °,  $\theta_{\min} = 2.0$ °

$h = -13 \rightarrow 13$

$k = -7 \rightarrow 7$

$l = -18 \rightarrow 18$

#### Refinement

Refinement on  $F^2$

Least-squares matrix: full

$R[F^2 > 2\sigma(F^2)] = 0.038$

$wR(F^2) = 0.098$

$S = 1.05$

1945 reflections

109 parameters

0 restraints

Hydrogen site location: inferred from  
neighbouring sites

H-atom parameters constrained

$w = 1/[\sigma^2(F_o^2) + (0.056P)^2 + 0.1275P]$   
where  $P = (F_o^2 + 2F_c^2)/3$

$(\Delta/\sigma)_{\max} < 0.001$

$\Delta\rho_{\max} = 0.39$  e Å<sup>-3</sup>

$\Delta\rho_{\min} = -0.36$  e Å<sup>-3</sup>

*Special details*

**Geometry.** All esds (except the esd in the dihedral angle between two l.s. planes) are estimated using the full covariance matrix. The cell esds are taken into account individually in the estimation of esds in distances, angles and torsion angles; correlations between esds in cell parameters are only used when they are defined by crystal symmetry. An approximate (isotropic) treatment of cell esds is used for estimating esds involving l.s. planes.

*Fractional atomic coordinates and isotropic or equivalent isotropic displacement parameters ( $\text{\AA}^2$ )*

	<i>x</i>	<i>y</i>	<i>z</i>	$U_{\text{iso}}^*/U_{\text{eq}}$
Ni1	0.500000	0.29112 (8)	0.750000	0.03467 (16)
N1	0.3260 (3)	0.2587 (4)	0.70613 (16)	0.0416 (6)
C1	0.2221 (3)	0.1954 (5)	0.67755 (18)	0.0375 (6)
S1	0.07891 (8)	0.10731 (15)	0.63716 (6)	0.0536 (2)
S11	0.51467 (7)	0.31221 (13)	0.60612 (5)	0.0421 (2)
C11	0.6634 (3)	0.4138 (5)	0.60210 (18)	0.0368 (6)
N11	0.7271 (2)	0.3274 (4)	0.54463 (16)	0.0402 (5)
C12	0.7000 (4)	0.1112 (6)	0.5071 (2)	0.0551 (8)
H12A	0.658143	0.026358	0.546631	0.083*
H12B	0.780347	0.041141	0.502878	0.083*
H12C	0.643405	0.121046	0.446582	0.083*
C13	0.8112 (3)	0.4537 (6)	0.5012 (2)	0.0495 (8)
H13A	0.801002	0.607219	0.513061	0.074*
H13B	0.788670	0.427747	0.435733	0.074*
H13C	0.900282	0.410930	0.525696	0.074*
N12	0.7143 (2)	0.5845 (4)	0.65156 (16)	0.0410 (5)
C14	0.6379 (4)	0.7320 (5)	0.6929 (2)	0.0522 (8)
H14A	0.549871	0.735359	0.656431	0.078*
H14B	0.674874	0.876929	0.695780	0.078*
H14C	0.637766	0.682513	0.754302	0.078*
C15	0.8524 (3)	0.6057 (6)	0.6875 (2)	0.0522 (8)
H15A	0.894942	0.470956	0.677642	0.078*
H15B	0.869414	0.636391	0.752599	0.078*
H15C	0.885381	0.723850	0.656457	0.078*

*Atomic displacement parameters ( $\text{\AA}^2$ )*

	$U^{11}$	$U^{22}$	$U^{33}$	$U^{12}$	$U^{13}$	$U^{23}$
Ni1	0.0307 (3)	0.0413 (3)	0.0316 (3)	0.000	0.00619 (19)	0.000
N1	0.0423 (15)	0.0489 (14)	0.0335 (12)	0.0005 (11)	0.0085 (10)	0.0004 (10)
C1	0.0364 (16)	0.0446 (15)	0.0319 (13)	0.0021 (12)	0.0086 (11)	0.0017 (11)
S1	0.0354 (4)	0.0637 (5)	0.0597 (5)	-0.0076 (4)	0.0063 (4)	-0.0022 (4)
S11	0.0360 (4)	0.0576 (5)	0.0323 (4)	-0.0074 (3)	0.0069 (3)	-0.0023 (3)
C11	0.0337 (14)	0.0430 (14)	0.0327 (13)	0.0007 (12)	0.0052 (11)	0.0045 (11)
N11	0.0399 (13)	0.0451 (13)	0.0368 (12)	0.0015 (10)	0.0112 (10)	0.0024 (10)
C12	0.066 (2)	0.0556 (19)	0.0474 (18)	-0.0026 (17)	0.0204 (16)	-0.0084 (15)
C13	0.0405 (17)	0.065 (2)	0.0471 (17)	0.0022 (15)	0.0188 (14)	0.0113 (14)
N12	0.0391 (13)	0.0417 (13)	0.0418 (13)	-0.0021 (10)	0.0081 (10)	-0.0029 (10)
C14	0.060 (2)	0.0426 (16)	0.0564 (19)	0.0031 (14)	0.0185 (16)	-0.0051 (14)

C15	0.0418 (17)	0.0580 (19)	0.0539 (18)	-0.0090 (15)	0.0050 (14)	-0.0051 (15)
-----	-------------	-------------	-------------	--------------	-------------	--------------

*Geometric parameters (Å, °)*

Ni1—N1	1.844 (3)	C11—N12	1.340 (4)
Ni1—S11	2.2259 (7)	N11—C13	1.460 (4)
N1—C1	1.168 (4)	N11—C12	1.460 (4)
C1—S1	1.614 (3)	N12—C14	1.461 (4)
S11—C11	1.729 (3)	N12—C15	1.464 (4)
C11—N11	1.335 (4)		
N1—Ni1—N1 <sup>i</sup>	167.47 (16)	N11—C11—S11	119.3 (2)
N1—Ni1—S11	86.80 (8)	N12—C11—S11	122.0 (2)
N1 <sup>i</sup> —Ni1—S11	93.93 (8)	C11—N11—C13	122.6 (3)
S11 <sup>i</sup> —Ni1—S11	173.26 (5)	C11—N11—C12	122.5 (3)
C1—N1—Ni1	166.5 (3)	C13—N11—C12	113.9 (2)
N1—C1—S1	179.4 (3)	C11—N12—C14	122.6 (3)
C11—S11—Ni1	109.10 (9)	C11—N12—C15	121.9 (3)
N11—C11—N12	118.6 (3)	C14—N12—C15	113.7 (3)

Symmetry code: (i)  $-x+1, y, -z+3/2$ .*Hydrogen-bond geometry (Å, °)*

<i>D</i> —H $\cdots$ <i>A</i>	<i>D</i> —H	H $\cdots$ <i>A</i>	<i>D</i> $\cdots$ <i>A</i>	<i>D</i> —H $\cdots$ <i>A</i>
C12—H12B $\cdots$ S1 <sup>ii</sup>	0.98	3.01	3.821 (3)	140
C13—H13C $\cdots$ S1 <sup>iii</sup>	0.98	2.93	3.798 (3)	148

Symmetry codes: (ii)  $-x+1, -y, -z+1$ ; (iii)  $x+1, y, z$ .